

# A Plug-and-Play Deep Denoiser Prior Model for Accelerated MRI Reconstruction

Hasan H. Karaoglu, and Ender M. Eksioğlu  
Electronics and Communication Engineering Department  
Istanbul Technical University  
Istanbul, Turkey  
karaoglu.hasan, eksioglue@itu.edu.tr

**Abstract**—Magnetic resonance imaging (MRI) reconstruction is one of the important inverse imaging problems. Unlike the classical MRI approaches which demand long scanning time and are prone to reconstruction artifacts, compressed sensing MRI (CS-MRI) generates the scans data relatively faster and produces less artifacts for medical diagnosis. Model-based CS-MRI algorithms require long reconstruction time to obtain an MR image. On the other hand, although training time of deep learning techniques for the task is rather long, their reconstruction time is much shorter compared to iterative model-based MRI algorithms. Moreover, recent works have shown that Gaussian denoisers including deep denoisers can be utilized to solve the inverse problems in a plug-and-play fashion. In this paper, we propose an iterative convolutional neural network based Gaussian denoiser as a solver for the CS-MRI problem. Our experiments show that the proposed method has better reconstruction ability when compared to some important model-based and deep learning based methods from the literature.

**Keywords**—Compressed sensing; deep learning; denoiser prior; image reconstruction; magnetic resonance imaging

## I. INTRODUCTION

Inverse problems in imaging target to recover or reconstruct a latent signal  $\mathbf{x}$  from an observed signal  $\mathbf{y}$ . The forward observation model for an inverse imaging problem can be formulated by the following equation

$$\mathbf{y} = \mathbf{H}\mathbf{x} + \boldsymbol{\eta}. \quad (1)$$

Here,  $\mathbf{H}$  is a linear degradation operator and  $\boldsymbol{\eta}$  is an additive noise. Notice that the observed signal  $\mathbf{y}$ , the latent signal  $\mathbf{x}$ , and the noise  $\boldsymbol{\eta}$  are vectorized in a lexicographical order. If the operator  $\mathbf{H}$  is chosen as an identity matrix, the problem is termed as image denoising. If  $\mathbf{H}$  is a convolution matrix, Eq. 1 is called image deconvolution. If the problem of interest is MRI, the corresponding  $\mathbf{H}$  operator is subsampled Fourier matrix. Inverse problems in imaging typically ill-posed problems [1]. Ill-posedness means the solution may not exist, it may not be unique or it is sensitive to small variations in observation. In order to solve an ill-posed inverse problem efficiently, regularizing the problem is of paramount importance. It is well known that regularization corresponds to prior modeling in the stochastic domain [2]. From the Bayesian viewpoint, the

solution can be found by solving the following optimization problem

$$\hat{\mathbf{x}} = \arg \min_{\mathbf{x}} \frac{1}{2} \|\mathbf{y} - \mathbf{H}\mathbf{x}\|^2 + \tau \mathbf{R}(\mathbf{x}). \quad (2)$$

The above problem minimizes an objective function which consists of a data fidelity term  $\frac{1}{2} \|\mathbf{y} - \mathbf{H}\mathbf{x}\|^2$ , and a regularization term  $\mathbf{R}(\mathbf{x})$ . Hyperparameter  $\tau$  is called as regularization parameter, and it leads to a tradeoff between the data fidelity and regularization terms in the objective function of Eq. 2. While the fidelity term of the objective function enforces the solution to match with the observed data, the regularization term enforces the model prior on the solution. Among popular and widely used priors in both image restoration and inverse problem communities we can list sparsity, low-rankness and non-local self-similarity priors as important examples [3]. These priors are well-designed priors whose inspiration have been taken from natural images and require domain expertise.

Magnetic resonance imaging (MRI), a popular member of the inverse problem family, has a wide area of application in clinical studies. MRI allows us non-invasive, and quantitative measurements of tissue, including anatomical and structural information. Since MR data are measured in k-space (the Fourier domain), one fundamental challenge of MRI modality is long acquisition time. The other drawbacks are the inherent motion and contrast artifacts.

Compressed sensing (CS) targets to reconstruct any signal from much fewer measurements than the Nyquist-Shannon sampling criteria. One of the fundamental application area of CS is magnetic resonance imaging due to lower measurements, fast acquisition and less artifacts. This fast MRI problem is called as compressed sensing or accelerated MRI in the medical imaging literature.

Typically, CS-MRI problem can be formulated as in Eq. 3 if we substitute  $\mathbf{H}$  for subsampled Fourier matrix  $\mathcal{F}_{\mathbf{u}}$

$$\min_{\mathbf{x}} \frac{1}{2} \|\mathbf{y} - \mathcal{F}_{\mathbf{u}}\mathbf{x}\|_2^2 + \tau \mathbf{R}(\mathbf{x}). \quad (3)$$

Before the deep learning era, model-based methods have attained great success for CS-MRI task. As a first successful algorithm for compressed sensing MRI, Sparse-MRI [4] uses the Total Variation seminorm as a prior in the objective function in Eq.3. PANO [5] (Patch-based Nonlocal Operator)

This work is supported by TUBITAK (The Scientific and Technological Research Council of Turkey) under project number 119E248.

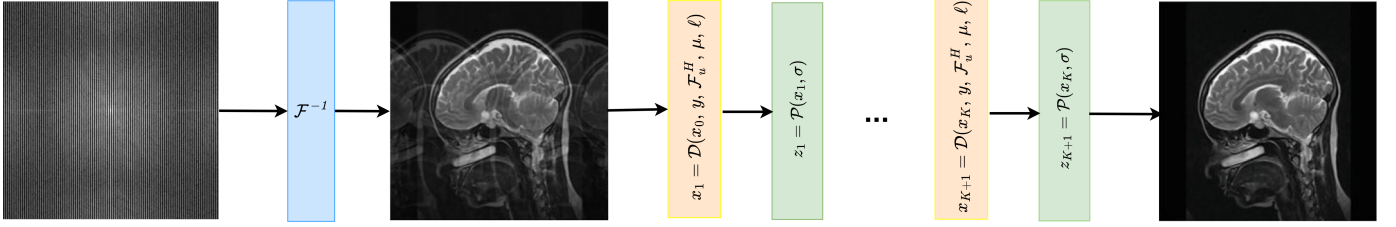


Fig. 1. Flowchart of the proposed method.  $\mathcal{F}^{-1}$ ,  $\mathcal{D}(\cdot)$ , and  $\mathcal{P}(\cdot)$  denote the inverse Fourier Transform operator, fidelity and denoiser prior modules, respectively.

proposes nonlocal self-similarity based prior for the task and achieves great success. BM3D-MRI [6], by making use of the well designed block matching 3D denoiser (BM3D) in a plug-and-play fashion, has been state-of-the-art image reconstruction algorithm in the MRI literature. However, model-based methods suffer from slow reconstruction speed due to the optimization procedure. Deep ADMM-Net [7] is a first and representative algorithm example of deep unrolling techniques which means each step and each operation in a successful iterative image reconstruction algorithm can be thought of as deep stages and deep layers. Deep ADMM-Net achieves highly competitive results for magnetic resonance imaging. Aside from ADMM-Net, DAGAN [8] and Deep Cascaded MRI [9] can be shown as the other successful deep learning based MRI methods.

Using the variable splitting techniques from the optimization literature such as the Half-Quadratic Splitting (HQS) and Alternating Direction Method of Multipliers (ADMM), the objective function in Eq.2 can be separated into two subproblems. While the first one, dubbed as the data fidelity subproblem, can be solved with the aid of least squares techniques, the latter one which is called prior subproblem can be solved with a Gaussian denoiser in an implicit manner. Inspired by this implicit solver step, we propose deep CNN denoiser prior to Eq. 3 instead of the regularization term  $\mathbf{R}(\cdot)$ . We choose a powerful deep Gaussian denoiser as the solver of the prior problem.

The main contribution of this work is to propose an iterative CNN-based Gaussian denoiser as the solver of the prior subproblem to reconstruct MR images. The proposed method achieves superior results to the deep-learning based and model-based algorithms.

## II. PLUG-AND-PLAY (PNP) DENOISERS

To make use of any denoiser prior in a plug-and-play fashion, numerous variable splitting techniques such as Alternating Direction Method of Multipliers (ADMM), Augmented Lagrangian Method (ALM), and Half-Quadratic Splitting (HQS) are utilized. By using these techniques, the objective function in Eq.3 is decoupled into two parts. In the method HQS, the function in Eq.3 is added an auxiliary variable  $\mathbf{z}$  as a constrained optimization problem as follows

$$\hat{\mathbf{x}} = \arg \min_{\mathbf{x}} \frac{1}{2} \|\mathbf{y} - \mathcal{F}_u \mathbf{x}\|^2 + \tau \mathbf{R}(\mathbf{z}) \quad \text{s.t.} \quad \mathbf{z} = \mathbf{x}. \quad (4)$$

Notice that Eq. 4 can be rewritten as an unconstrained optimization problem.

$$\mathcal{L}_\alpha(\mathbf{x}, \mathbf{z}) = \frac{1}{2} \|\mathbf{y} - \mathcal{F}_u \mathbf{x}\|^2 + \tau \mathbf{R}(\mathbf{z}) + \frac{\alpha}{2} \|\mathbf{z} - \mathbf{x}\|^2. \quad (5)$$

where  $\alpha$  is a penalty parameter which is a nonnegative number and varies in each iteration in a non-descending order. Eq. 5 can be divided into the following two subproblems:

$$\mathbf{x}_{k+1} = \arg \min_{\mathbf{x}} \|\mathbf{y} - \mathcal{F}_u \mathbf{x}\|^2 + \alpha \|\mathbf{x} - \mathbf{z}_k\|^2, \quad (6a)$$

$$\mathbf{z}_{k+1} = \arg \min_{\mathbf{z}} \frac{\alpha}{2} \|\mathbf{z} - \mathbf{x}_{k+1}\|^2 + \tau \mathbf{R}(\mathbf{z})., \quad (6b)$$

The equations 6a, and 6b are called data fidelity, and prior problems, respectively. Notice that the CS-MRI objective function in Eq. 3 is decoupled into two smaller objective functions, each of which will be optimized separately. The data fidelity subproblem can be considered as a regularized least-squares problem and a direct solution for this subproblem is obtained by

$$\mathbf{x}_{k+1} = \left( \mathcal{F}_u^H \mathcal{F}_u + \alpha \mathbf{I} \right)^{-1} \left( \mathcal{F}_u^H \mathbf{y} + \alpha \mathbf{z}_k \right). \quad (7)$$

where  $\mathcal{F}_u^H$  denotes the adjoint operator for the subsampled Fourier matrix  $\mathcal{F}_u$ . It is well known that the matrix  $\mathcal{F}_u$  can be diagonalized by the full Fourier transform matrix as follows:

$$\mathcal{F} \mathcal{F}_u^H \mathcal{F}_u \mathcal{F}^H = \Lambda \quad (8)$$

$\Lambda$  is a diagonal matrix with ones and zeros on its diagonal, operator  $\mathcal{F}$  is the full Fourier transform matrix which is also unitary matrix. The diagonal matrix  $\Lambda$  is only nonzero at the diagonal entries  $\ell \in \Omega$ , where  $\Omega$  denotes the set of indices for Fourier data included in the image  $\mathbf{y}$ . By utilizing the diagonalizability property of a subsampled Fourier matrix from Eq. 8, we obtain the following equation:

$$\mathcal{F} \hat{\mathbf{x}}_{k+1} = \begin{cases} \mathcal{F} \mathbf{x}_k & , \text{ if } \ell \notin \Omega \\ \frac{\mathcal{F} \mathcal{F}_u^H \mathbf{y} + \alpha \mathcal{F} \mathbf{x}_k}{1 + \alpha} & , \text{ if } \ell \in \Omega \end{cases} \quad (9)$$

Eq. 9 is the solution of the data fidelity subproblem in Eq. 6a. If Eq. 9 is written in an input-output relationship, we achieve the following symbolic formula

$$\mathbf{x}_{k+1} = \mathcal{D}(\mathbf{x}_k, \mathbf{y}, \mathcal{F}_u^H, \alpha, \ell). \quad (10)$$

Here,  $\mathcal{D}(\cdot)$  is the inverse Fourier Transform of Eq. 9 and called Data Fidelity Module.

TABLE I. QUANTITATIVE RESULTS ON BRAIN, HEAD AND BUST IMAGES WITH 20% SAMPLING RATES OF THE PSEUDO RADIAL SAMPLING MASK.

Method	Brain				Head				Bust			
	NMSE	PSNR	SSIM	Time	NMSE	PSNR	SSIM	Time	NMSE	PSNR	SSIM	Time
Zero Filling	0.1366	27.8488	0.5674	<b>0.001</b>	0.1524	26.1148	0.6278	<b>0.001</b>	0.2935	23.8083	0.4496	<b>0.001</b>
TV	0.0747	33.3192	0.8809	1.135	0.1138	28.8253	0.7796	1.052	0.1731	28.4468	0.7385	1.842
PANO	0.0612	35.1004	0.9265	46.592	0.0996	30.0037	0.8200	46.343	0.1455	29.9608	0.8386	73.044
BM3D-MRI	0.0506	36.7685	0.9477	18.067	<b>0.0856</b>	<b>31.3510</b>	<b>0.8628</b>	18.719	0.1128	32.2116	0.9263	18.454
ADMM-Net	0.0562	35.8272	0.9424	2.038	0.0925	30.6378	0.8505	1.996	0.1338	30.6630	0.8846	1.830
IRCNN-MRI	<b>0.0480</b>	<b>37.2286</b>	<b>0.9492</b>	11.577	0.0896	30.9532	0.8601	11.636	<b>0.1051</b>	<b>32.8249</b>	<b>0.9338</b>	14.093

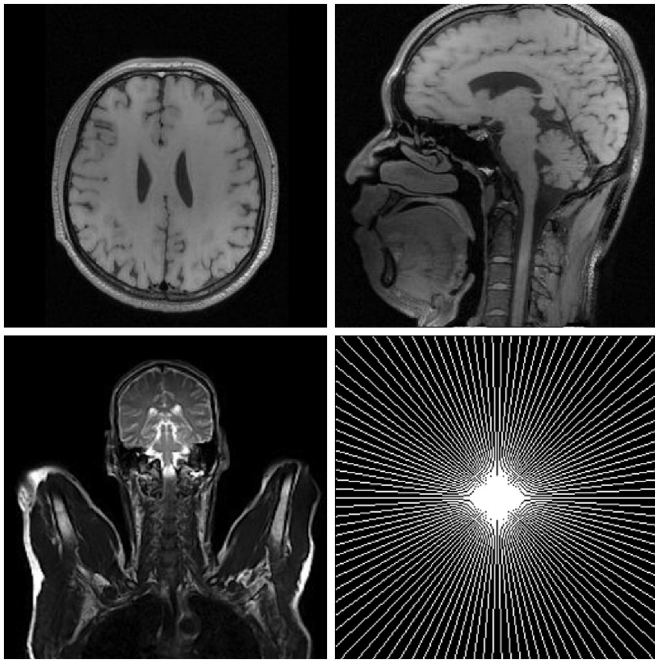


Fig. 2. Test images used in our simulations and 20% radial sampling mask shown at the bottom-right of the figure.

When we go back to Eq. 6b, it can be rewritten by

$$z_{k+1} = \arg \min_z \frac{1}{2(\sqrt{\tau/\alpha})^2} \|x_{k+1} - z\|^2 + R(z). \quad (11)$$

The work [10] suggest that Eq. 11 corresponds to denoising the image  $x_{k+1}$  by a Gaussian denoiser with the noise level  $\sqrt{\tau/\alpha}$ . The authors of the work term this type of denoiser as a Plug-and-Play (PnP) denoiser. By this paradigm, a powerful Gaussian denoiser can be used as the solver of Eq. 11. Like in Eq. 10, we can write Eq. 11 in the symbolic expression as follows:

$$z_{k+1} = \mathcal{P}(x_{k+1}, \sigma). \quad (12)$$

where  $\mathcal{P}(\cdot)$  denotes any Gaussian denoiser (model-based or learning-based) and is called Prior Module. Parameter  $\sigma = \sqrt{\tau/\alpha}$  is the noise level of the denoiser.

Utilizing the module expressions (10), and (12), the general block diagram of our proposed method can be illustrated in Fig.1. The zero-filled k-space data can be seen at the very left

of the block diagram. Our method takes the zero-filled image  $\mathcal{F}_u^H y$  of the measured signal  $y$  as the input and processes it iteratively passing through the data fidelity and prior modules.

### III. EXPERIMENTAL STUDY

In this part, we present and evaluate our PnP based deep denoiser model. As a denoiser which is based on deep learned models in the prior module, we select a vanilla CNN architecture which consists of seven layers. Except for the first and last layers, the remaining layers have the composite Convolution (Conv in short) + Batch Normalization (BNorm in short) + Rectified Linear Unit (ReLU in short) block. The first and the last layers include Conv + ReLU and Conv blocks, respectively. The network which were used has different dilation factors for each layer. Starting from the first layer to the last one, the dilation factors are determined as 1, 2, 3, 4, 3, 2, and 1, respectively. The number of feature maps in the middle layers is specified as 64. For the experiments in this paper, we directly use the publicly available models provided by the authors of [11] instead of retraining 25 denoisers from scratch which necessitates high compute resources and long computation time. The noise level  $\sigma$  of all the denoisers is determined incrementing by 2 on the interval between 2 and 50. In the proposed algorithm, we choose the regularization parameter  $\tau$  as  $8e^{-4}$ , determined after multiple experiments. We specified the iteration number  $K$  as 200. We set the parameter  $\alpha$  to the values from 49 to 1 in an exponentially decaying manner.

In the simulations, we pick three frequently used test images from the CS-MRI literature. The first image is T1-weighted brain image which is shown at the top left of Fig. 2. Our second test image reveals a brain image on the sagittal plane shown at the top right of Fig. 2. The final bust image is shown at the bottom left part of the same figure. All of the images used in the experiments are real and positive valued. The sampling in the Fourier domain is realized by using radial downsampling mask. The downsampling ratio is chosen as 20%. For our simulation setting, we assume that there is no observation noise.

The implementation of our proposed method has been performed by MatConvNet [12] package, Matlab based highly optimized deep learning package. All experiments were simulated in MATLAB (2019a) on a laptop computer with an Intel Core i7-4720k CPU, 64-bit operating system, and 8GB

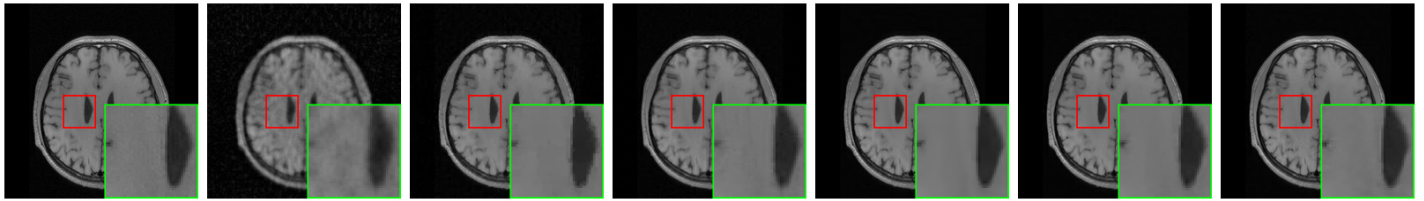


Fig. 3. Example reconstruction results on the brain data with 20% sampling rate. The images show the ground truth image, zero-filled image, TV [4], PANO [5], BM3D-MRI [6], ADMM-Net [7], and our, from the left to right.

memory and a GeForce GTX960 GPU. We have used the publicly available codes for all of the compared methods. We choose the Normalized Mean Square Error (NMSE), the Peak Signal-to-Noise Ratio (PSNR, measured in dB) and the Structural Similarity Index (SSIM) as the performance metrics of all the algorithms compared in this paper. Like many CS-MRI based settings, the reconstructed fully sampled k-space data were used as ground truth (GT) for validation. Zero-filled image was considered initial reconstructed image for all the methods in this paper.

We compare our proposed algorithm with some representative algorithms. Specifically, three model-based approaches, the TV method [4], the PANO method [5], and the BM3D-MRI method [6] and the ADMM-Net method [7], a deep learning based reconstruction algorithm, are utilized to compare with our proposed method. Note that BM3D-MRI and ADMM-Net algorithms are the powerful CS-MRI algorithms.

The measured NMSE, PSNR and SSIM results on the three MR test images are shown in Table I. From the table, one can infer that the proposed method outperforms all model based MRI methods but BM3D-MRI algorithm. The proposed method surpasses the BM3D-MRI algorithm in the brain and bust images by a large margin. However, in the head image, BM3D-MRI technique is superior to the proposed model by a relatively smaller margin. Visual results also prove the superiority of the proposed CNN denoiser based model as seen in Fig. 3. Our model can reconstruct the brain image with less artifacts. Due to the different algorithm implementations in various deep learning packages, our comparisons could not be extended to the other deep learning based CS-MRI algorithms. In the future work, we will get deeper our experiments for showing the superiority of the proposed method to the other deep learning algorithms.

#### IV. CONCLUSION

In this paper, we have proposed a PnP-based deep CNN denoiser model for reconstructing magnetic resonance images. Our model aims to incorporate a deep CNN denoiser as a subsolver of the reconstruction algorithm. For that purpose, firstly we designed a latent objective function incorporating deep CNN based Gaussian denoiser priors, and we provided an analysis of its optimization process using the HQS variable splitting technique. Then, by decoupling the prior terms and data fidelity terms as sub-problems, each problem is solved

on its own. While the data fidelity problem has a closed-form solution, the prior problem has been solved by a deep Gaussian denoiser implicitly. Finally, in order to validate the proposed models for the CS-MRI task, numerous experiments were conducted. The quantitative and qualitative results have shown that our method has given the best performance when compared with some state-of-the-art model-based and learning-based algorithms.

#### REFERENCES

- [1] A. Ribes and F. Schmitt, "Linear Inverse Problems in Imaging," *IEEE Signal Processing Magazine*, vol. 25, no. 4, pp. 84–99, 2008.
- [2] C. M. Bishop, *Pattern Recognition and Machine Learning*. Springer, 2006.
- [3] L. Zhang and W. Zuo, "Image Restoration: From Sparse and Low-Rank Priors to Deep Priors [Lecture Notes]," *IEEE Signal Processing Magazine*, vol. 34, no. 5, pp. 172–179, 2017.
- [4] M. Lustig, D. Donoho, and J. M. Pauly, "Sparse MRI: The Application of Compressed Sensing for Rapid MR Imaging," *Magnetic Resonance in Medicine: An Official Journal of the International Society for Magnetic Resonance in Medicine*, vol. 58, no. 6, pp. 1182–1195, 2007.
- [5] X. Qu, Y. Hou, F. Lam, D. Guo, J. Zhong, and Z. Chen, "Magnetic Resonance Image Reconstruction from Undersampled Measurements using a Patch-based Nonlocal Operator," *Medical Image Analysis*, vol. 18, no. 6, pp. 843–856, 2014.
- [6] E. M. Eksioğlu, "Decoupled Algorithm for MRI Reconstruction using Nonlocal Block Matching Model: BM3D-MRI," *Journal of Mathematical Imaging and Vision*, vol. 56, no. 3, pp. 430–440, 2016.
- [7] J. Sun, H. Li, Z. Xu *et al.*, "Deep ADMM-Net for Compressive Sensing MRI," *Advances in Neural Information Processing Systems*, vol. 29, 2016.
- [8] G. Yang, S. Yu, H. Dong, G. Slabaugh, P. L. Dragotti, X. Ye, F. Liu, S. Arridge, J. Keegan, Y. Guo, and D. Firmin, "DAGAN: Deep De-Aliasing Generative Adversarial Networks for Fast Compressed Sensing MRI Reconstruction," *IEEE Transactions on Medical Imaging*, vol. 37, no. 6, pp. 1310–1321, 2018.
- [9] J. Schlemper, J. Caballero, J. V. Hajnal, A. Price, and D. Rueckert, "A Deep Cascade of Convolutional Neural Networks for MR Image Reconstruction," in *International Conference on Information Processing in Medical Imaging*. Springer, 2017, pp. 647–658.
- [10] S. V. Venkatakrishnan, C. A. Bouman, and B. Wohlberg, "Plug-and-Play Priors for Model Based Reconstruction," in *2013 IEEE Global Conference on Signal and Information Processing*, 2013, pp. 945–948.
- [11] K. Zhang, W. Zuo, S. Gu, and L. Zhang, "Learning Deep CNN Denoiser Prior for Image Restoration," in *Proceedings of the IEEE Conference on Computer Vision and Pattern Recognition*, 2017, pp. 3929–3938.
- [12] A. Vedaldi and K. Lenc, "MatConvNet: Convolutional Neural Networks for Matlab," in *Proceedings of the 23rd ACM International Conference on Multimedia*, 2015, pp. 689–692.